Supplementary Information

Membrane-dependent Signal Integration by the Ras Activator Son of Sevenless

Jodi Gureasko, William J. Galush, Sean Boykevisch, Holger Sondermann,
Dafna Bar-Sagi, Jay T. Groves and John Kuriyan

Supplementary Methods

Liposome Binding Assays

The binding of SOS proteins to phospholipid vesicles composed of a mixture of phosphatidylcholine (PC), phosphatidylserine (PS) and the relevant phospholipid species at ratios of 80:10:10 was assayed using flotation through a sucrose density gradient to separate protein-associated vesicles from free protein[1]. Phospholipid vesicles (10 μg total lipid, corresponding to ~20 μM lipid of interest) were incubated with SOS proteins (1 ng) at room temperature for 20 min. Binding reactions were mixed with 50 μl of 2.5 M sucrose in binding buffer (25 mM HEPES-NaOH [pH 7.4] and 100 mM NaCl) to make a final concentration of 1.0 M sucrose. A 100 μl sample of this mixture was layered onto the bottom of a polycarbonate (7 × 20 mm) centrifuge tube (Beckman) and overlaid with 100 μl of 0.75 M sucrose in binding buffer followed by 20 μl of binding buffer. Centrifugation was carried out at 100,000 × g for 20 min at room temperature in a TLA100 rotor (Beckman). Phospholipid vesicles were recovered by flotation through the gradient and phospholipid-associated proteins were analyzed using SDS–PAGE followed by silver staining (SilverQuest, Invitrogen) after normalizing for lipid recovery.

Supplementary Table 1

Calculation of Ras molecules per vesicle and Ras surface density (molecules μm^{-2})

mol% Ras-coupled maleimide-lipids∗	Number of Ras molecules per vesicle	Surface density per vesicle (Ras μm^{-2})
0.1	39	1300
0.3	117	3900
0.6	234	7800

∗ mol% Ras-coupled maleimide-lipids is calculated using final protein and lipid concentrations after Ras-conjugation (see Methods).

The number of Ras molecules per vesicle and the surface density of Ras (Ras molecules per μm^2) are calculated based on the following assumptions:

- Radius of vesicle ≈ 50 nm, surface area of vesicle = $4\pi r^2 \approx 3 \times 10^4$ nm^2 (≈ 0.03 μm^2)
- Surface area of lipid ≈ 0.8 nm^2, number of surface lipids per vesicle ≈ 3.9×10^4
- Number of Ras molecules per vesicle = (mol% Ras-coupled lipids/100)×(surface lipids/vesicle) ≈ $(0.001)\times(3.9 \times 10^4)$ ≈ 39 Ras molecules/vesicle
- Surface density of Ras molecules per μm^2 = (Ras molecules/vesicle)/(surface area of vesicle) ≈ (39 Ras/vesicle)/(0.03 μm^2/vesicle) ≈ 1300 Ras/μm^2

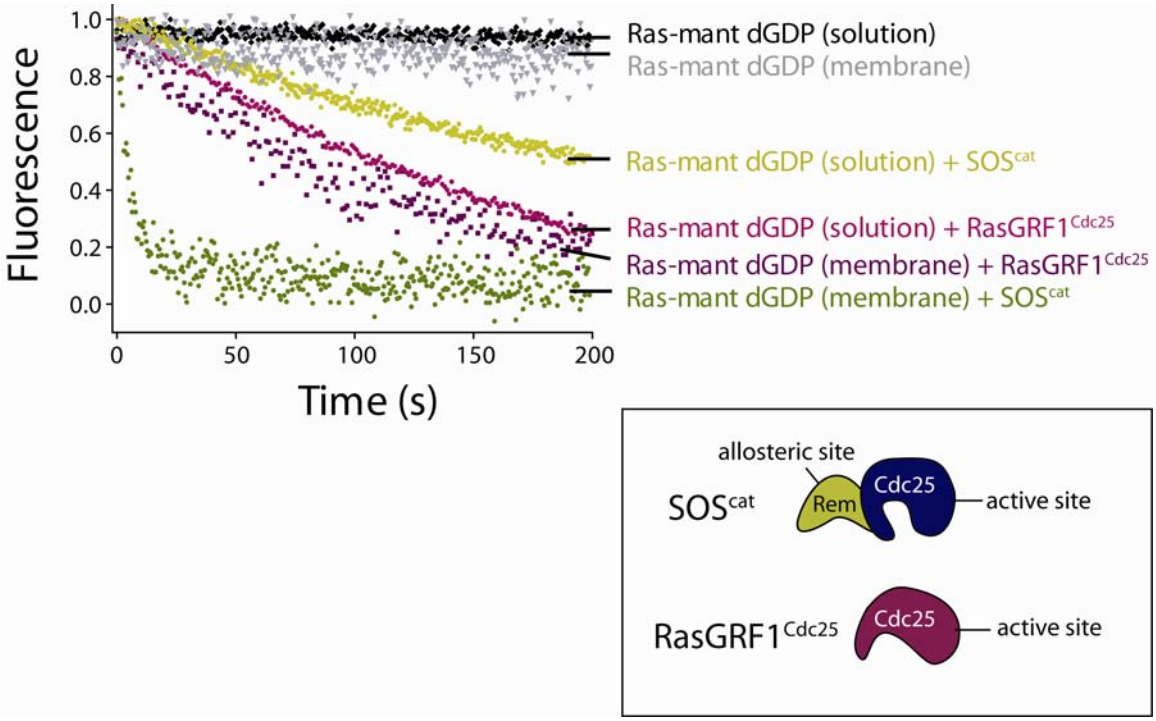

Supplementary Figure 1 Lipid attachment does not affect the intrinsic nucleotide release rates from Ras. To ensure that membrane anchorage of Ras does not alter the intrinsic rate of nucleotide release, we took advantage of an isolated Cdc25 domain construct of the SOS homolog Ras Guanine Nucleotide Releasing Factor 1 (RasGRF1), which is active in the absence of an allosteric activator[2]. The rate of fluorescently labeled mant-dGDP release from Ras in solution and membrane-bound Ras (~2,600 molecules μm^{-2}) in the presence of SOS^{cat} and $RasGRF1^{Cdc25}$ is compared (mant-dGDP exchanged for GDP). The bulk volume concentration of Ras, $RasGRF1^{Cdc25}$, and SOS^{cat} is 1 μM (when present). Note that membrane attachment does not alter the intrinsic nucleotide release rate from Ras alone or the $RasGRF1^{Cdc25}$-catalyzed rate.

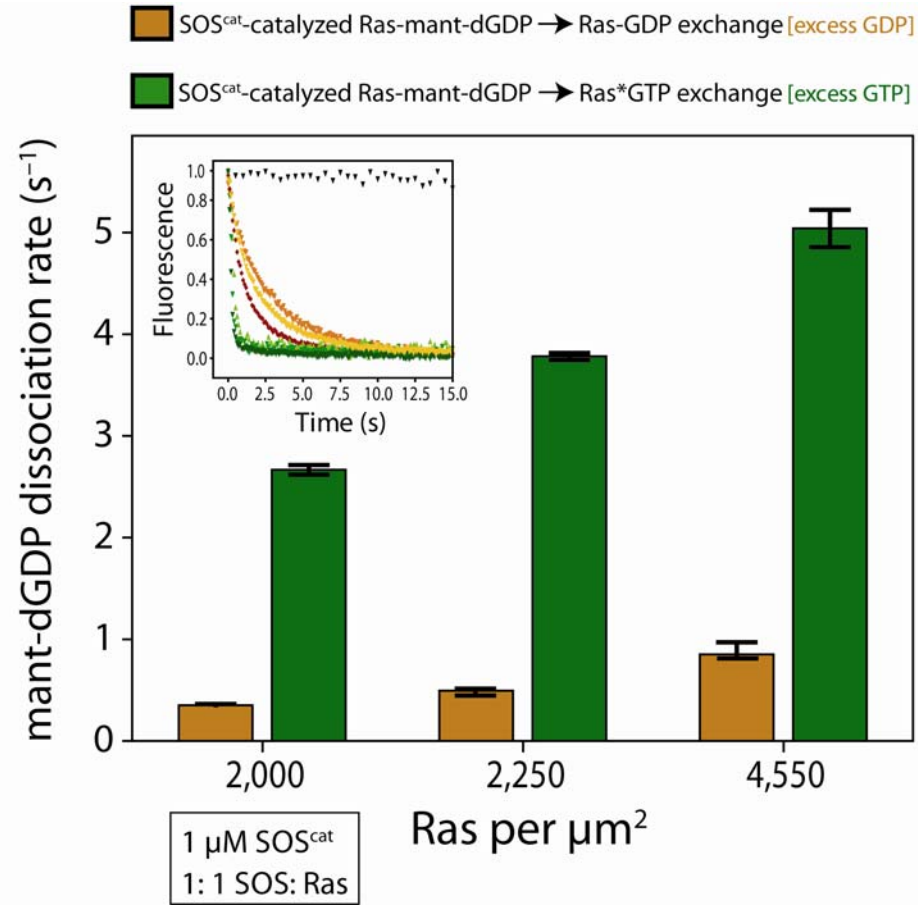

Supplementary Figure 2 The enhanced affinity of Ras-GTP for the allosteric site of SOS underlies the positive feedback activation of Ras by SOS. The rates for SOS^{cat}-catalyzed nucleotide exchange for Ras coupled to lipid vesicles when fluorescently labeled mant-dGDP is exchanged for either unlabeled GDP or GTP are compared for a given surface density of Ras. Although the rates are shown for three Ras surface densities, the bulk volume concentrations of Ras and SOS are the same for each measurement (1 μM). Note that the replacement of GDP for GTP on Ras results in a ~10-fold increase in the rate of SOS^{cat}-catalyzed nucleotide release for an equal surface density of membrane-bound Ras.

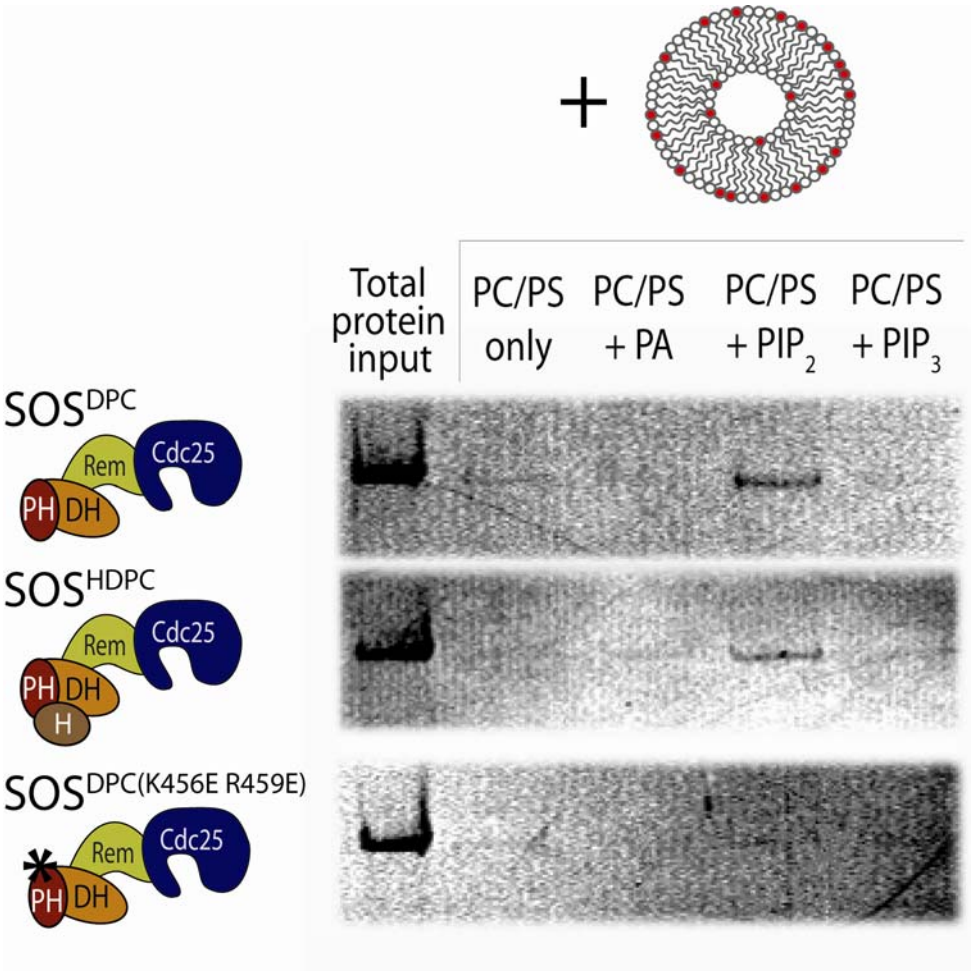

Supplementary Figure 3 PH domain-dependent binding of SOS to PIP_2. The binding of SOS proteins to lipid vesicles composed of a mixture of phosphatidylcholine (PC), phosphatidylserine (PS) and the relevant phospholipid species at ratios of 80:10:10 is assayed using a sucrose density gradient flotation assay (see Supplementary Methods). Binding of the PH domain containing SOS constructs, SOS^{DPC} and SOS^{HDPC}, to vesicles containing PIP_2 is observed. No binding to vesicles containing PIP_2 is observed for a mutant form of SOS^{DPC}, $SOS^{DPC(K456E\ R459E)}$, in which the two basic residues that are critical for PIP_2 binding are replaced by glutamate. The results shown are representative of five independent experiments.

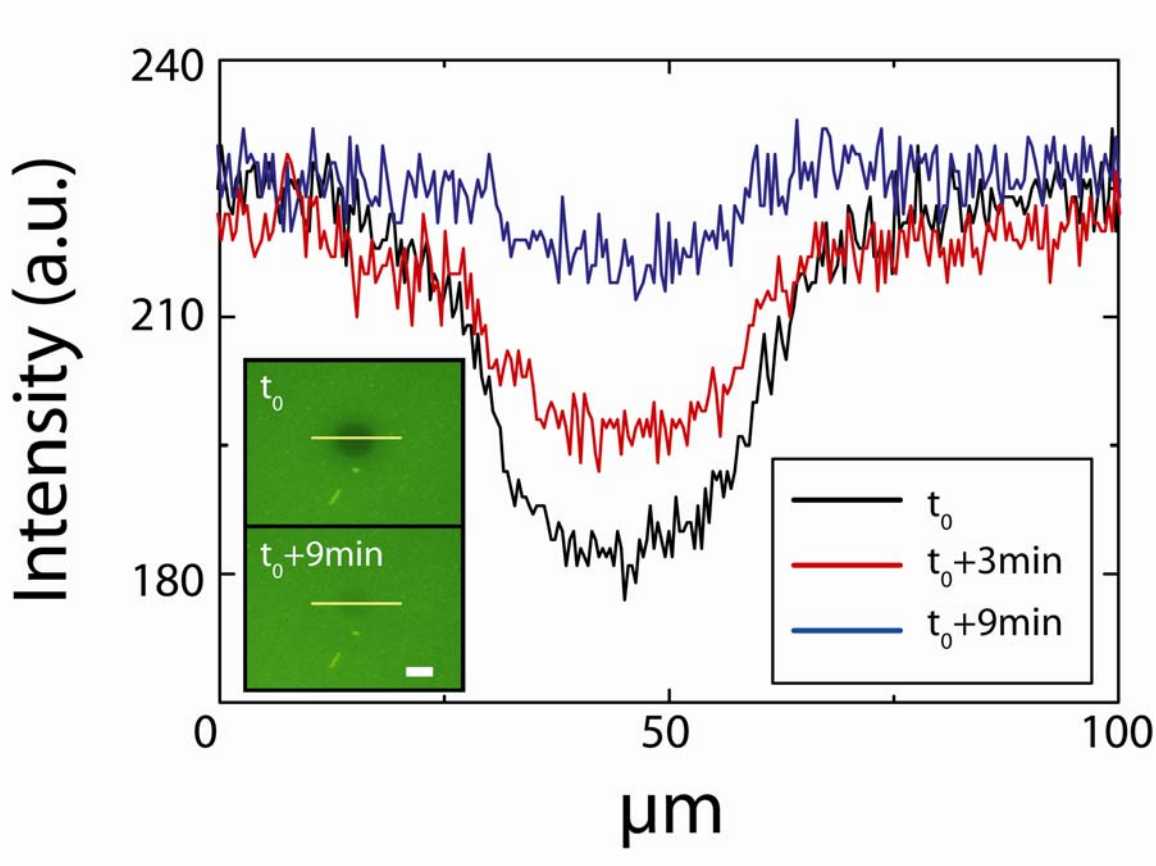

Supplementary Figure 4 Lateral mobility of Ras-coupled supported lipid bilayers. Membrane-linked Ras mobility is detected by fluorescence recovery after photobleaching (FRAP) experiments. High intensity illumination is used to bleach a small region of the membrane, bleaching most of the BODIPY-GDP fluorophores. After 9 minutes the bleached fluorophores have laterally diffused out of the spot, as indicated by intensity traces along the yellow line. [White bar = 20 μm]

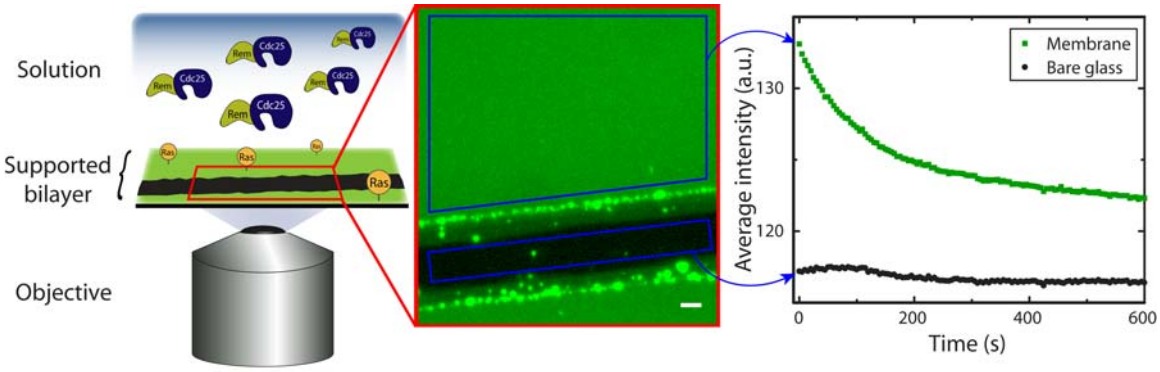

Supplementary Figure 5 Schematic of supported lipid bilayer experimental setup. A planar bilayer in a 400 μl well presents mobile, lipid-linked Ras to the solution (left). A small region of bilayer is removed by scratching with a needle (center, bar = 100 μm). Upon addition of SOS, signal from the bilayer decays with time, while the scratched region controls for signal from fluorescent nucleotide in solution (right).

Supplementary Discussion

Ras/SOS reaction network model

A model was constructed to simulate the interaction of membrane-bound Ras with SOS, where SOS is able to bind two Ras molecules, but only catalyzes nucleotide exchange at the catalytic site. We use a convention where "*Ras·SOS"* indicates Ras bound in the allosteric site, "*SOS·Ras"* indicates Ras bound in the catalytic site, and "*Ras·SOS·Ras*" indicates Ras in both allosteric and catalytic sites. The Ras-bound nucleotide is indicated by a "*" or "^{0}", where *Ras** is a protein loaded with fluorescent nucleotide, and Ras^0 is a protein with non-fluorescent nucleotide. Our model contains the following reactions:

$$Ras^* + SOS \underset{k_{-A0}}{\overset{k_{A0}}{\Leftrightarrow}} Ras^* \cdot SOS$$

$$SOS + Ras^* \underset{k_{-C0}}{\overset{k_{C0}}{\Leftrightarrow}} SOS \cdot Ras^*$$

$$Ras^* \cdot SOS + Ras^* \underset{k_{-C1}}{\overset{k_{C1}}{\Leftrightarrow}} Ras^* \cdot SOS \cdot Ras^*$$

$$Ras^* + SOS \cdot Ras^* \underset{k_{-A1}}{\overset{k_{A1}}{\Leftrightarrow}} Ras^* \cdot SOS \cdot Ras^*$$

$$Ras^0 + SOS \underset{k_{-A0}}{\overset{k_{A0}}{\Leftrightarrow}} Ras^0 \cdot SOS$$

$$SOS + Ras^0 \underset{k_{-C0}}{\overset{k_{C0}}{\Leftrightarrow}} SOS \cdot Ras^0$$

$$Ras^0 \cdot SOS + Ras^0 \underset{k_{-C1}}{\overset{k_{C1}}{\Leftrightarrow}} Ras^0 \cdot SOS \cdot Ras^0$$

$$Ras^0 + SOS \cdot Ras^0 \underset{k_{-A1}}{\overset{k_{A1}}{\Leftrightarrow}} Ras^0 \cdot SOS \cdot Ras^0$$

$$Ras^* \cdot SOS + Ras^0 \underset{k_{-C1}}{\overset{k_{C1}}{\Leftrightarrow}} Ras^* \cdot SOS \cdot Ras^0$$

$$Ras^0 + SOS \cdot Ras^* \underset{k_{-A1}}{\overset{k_{A1}}{\Leftrightarrow}} Ras^0 \cdot SOS \cdot Ras^*$$

$$Ras^0 \cdot SOS + Ras^* \underset{k_{-C1}}{\overset{k_{C1}}{\Leftrightarrow}} Ras^0 \cdot SOS \cdot Ras^*$$

$$Ras^{*} + SOS \cdot Ras^{0} \underset{k_{-A1}}{\overset{k_{A1}}{\Leftrightarrow}} Ras^{*} \cdot SOS \cdot Ras^{0}$$

$$Ras^{*} \cdot SOS \cdot Ras^{*} \xrightarrow{k_{fast}} Ras^{*} \cdot SOS \cdot Ras^{0}$$

$$SOS \cdot Ras^{*} \xrightarrow{k_{slow}} SOS \cdot Ras^{0}$$

$$Ras^{0} \cdot SOS \cdot Ras^{*} \xrightarrow{k_{fast}} Ras^{0} \cdot SOS \cdot Ras^{0}$$

where the rate constants are:

k_{A0} = binding to allosteric site (empty catalytic site)
k_{-A0} = unbinding from allosteric site (empty catalytic site)
k_{C0} = binding to catalytic site (empty allosteric site)
k_{-C0} = unbinding from catalytic site (empty allosteric site)
k_{A1} = binding to allosteric site (filled catalytic site)
k_{-A1} = unbinding from allosteric site (filled catalytic site)
k_{C1} = binding to catalytic site (filled allosteric site)
k_{-C1} = unbinding from catalytic site (empty allosteric site)
k_{slow} = nucleotide exchange rate constant with no allosteric Ras bound
k_{fast} = nucleotide exchange rate constant with allosteric Ras bound

and the "*0*" or "*1*" subscripts indicate the absence or presence, respectively, of Ras in the *nonexchanging*, allosteric binding site. Thus, k_{A0} is the forward rate constant to bind Ras to the allosteric site of SOS, while k_{A1} is the forward rate constant for Ras binding to the allosteric site of SOS·Ras (i.e. SOS with a Ras already in the catalytic site). All rate constants have units of s^{-1} (discussed below). Variables k_{fast} and k_{slow} are pseudo-first order constants for an excess of unlabeled nucleotide.

In order to have a unified scheme that deals with both solution and membrane-bound components, we consider all species and rates in terms of the absolute number of molecules rather than their volume or surface concentrations.

Thus, for unimolecular reactions, rates are expressed in the form

$$\frac{dx_i}{dt} = x_i k_l \qquad (1)$$

where x_i is number of molecules i and k_l is the rate constant for the reaction in units of s^{-1}.

For bimolecular interactions, the rate of reaction of species x_i is simply proportional to: i) the number x_i, ii) the probability of encountering a molecule of type j, and iii) a rate constant establishing the probability of the reaction occurring. This leads to bimolecular reaction rates of the form

$$\frac{dx_i}{dt} = x_i P_{x_j} k_l \tag{2}$$

where x_i is number of molecules i, P_{xj} is the probability of encountering a molecule of species j (given by j's volume or area fraction of the maximum close-packed density), and the rate constant k_l in units of s^{-1}. It is important to note that this analysis avoids the need to consider rate constants of mixed dimensionality that relate interactions between solution and surface species. Additionally, all rate constants are directly intercomparable, regardless of what chemical components are involved.

As a matter of clarification, the forward bimolecular reaction $i + j \rightarrow Product$ is often expressed as

$$\frac{d[C_i]}{dt} = C_i C_j k_{molar} \tag{3}$$

where C_i is the usual molar concentration of i, and k_{molar} is the usual molar bimolecular rate constant. Note that the left-hand side of (3) can be re-expressed as

$$\frac{d[C_i]}{dt} = \frac{d}{dt}\left(\frac{x_i}{N_A V}\right) \tag{4}$$

$$= \frac{dx_i}{dt}\frac{1}{N_A V} \tag{5}$$

where x_i is the number of molecules of i, N_A is Avogadro's number and V is the volume (assumed to be 1 liter).

Our molecular-based formalism applied to the same bimolecular reaction given by equation (2) can be written as

$$\frac{dx_i}{dt} = x_i \frac{x_j}{x_{j\max}} k_l \tag{6}$$

where $x_{j\max}$ is the maximum close packed number of j in 1 liter and k_l is once again the forward rate constant in units of s^{-1}.

Combining equations (5) and (6),

$$\frac{d[C_i]}{dt} = \frac{1}{N_A V} x_i \frac{x_j}{x_{j\max}} k_l = \left(\frac{x_i}{N_A V}\right)\left(\frac{x_j}{N_A V}\right) k_{molar} \tag{7}$$

so,

$$k_l\left(\frac{N_A V}{x_{j\max}}\right) = k_{molar} \qquad (8)$$

As an example, converting the value of k_{A0} below into molar concentration terms, one finds that the dissociation constant for Ras binding to the allosteric site (k_{-A0}/k_{A0}) is in the micromolar range.

We chose rate constants for the simulation that qualitatively describe the rate phenomena present in both vesicle and supported bilayer experiments. We have observed that BODIPY-GDP exchanges several fold faster than mant-dGDP, thus we set the rate constant of nucleotide exchange on supported bilayers to 3X the value used for vesicle simulations. We chose this ratio to best describe the behavior of both systems. The specific rate constants chosen were:

$k_{A0} = 48000\ s^{-1}$
$k_{-A0} = 12\ s^{-1}$
$k_{C0} = 0\ s^{-1}$
$k_{-C0} = 10^{10}\ s^{-1}$
$k_{A1} = 48000\ s^{-1}$
$k_{-A1} = 12\ s^{-1}$
$k_{C1} = 1000\ s^{-1}$
$k_{-C1} = 400\ s^{-1}$
$k_{slow} = 0\ s^{-1}$
$k_{fast} = 25\ s^{-1}$ (vesicle); $75\ s^{-1}$ (supported bilayer)

The above model leads to the following eleven differential equations, which were solved using Matlab (MathWorks) for the real experimental conditions for both the vesicle and supported bilayer systems. We analyzed the behavior of the sum of the fluorescent Ras species with respect to time to simulate the experimental observable. The term P_{xj} (the probability of molecule i encountering molecule j) is the volume fraction of j, given by x_j divided by $x_{j\max}$, where $x_{j\max}$ is the maximum close packed number of j in the volume or area.

$$\frac{dx_1}{dt} = -x_1\frac{x_2}{x_{2\max}}k_{A0} + x_3k_{-A0} - x_1\frac{x_2}{x_{2\max}}k_{C0} + x_4k_{-C0} - x_1\frac{x_3}{x_{3\max}}k_{C1} + x_5k_{-C1} - x_1\frac{x_4}{x_{4\max}}k_{A1} + x_5k_{-A1}$$
$$- x_1\frac{x_7}{x_{7\max}}k_{C1} + x_{11}k_{-C1} - x_1\frac{x_8}{x_{8\max}}k_{A1} + x_{10}k_{-A1}$$

$$\frac{dx_2}{dt} = -x_1\frac{x_2}{x_{2\max}}k_{A0} + x_3k_{-A0} - x_1\frac{x_2}{x_{2\max}}k_{C0} + x_4k_{-C0} - x_6\frac{x_2}{x_{2\max}}k_{A0} + x_7k_{-A0} - x_6\frac{x_2}{x_{2\max}}k_{C0} + x_8k_{-C0}$$

$$\frac{dx_3}{dt} = x_1\frac{x_2}{x_{2\max}}k_{A0} - x_3k_{-A0} - x_1\frac{x_3}{x_{3\max}}k_{C1} + x_5k_{-C1} - x_6\frac{x_3}{x_{3\max}}k_{C1} + x_{10}k_{-C1}$$

$$\frac{dx_4}{dt} = x_1 \frac{x_2}{x_{2\max}} k_{C0} - x_4 k_{-C0} - x_1 \frac{x_4}{x_{4\max}} k_{A1} + x_5 k_{-A1} - x_6 \frac{x_4}{x_{4\max}} k_{A1} + x_{11} k_{-A1} - x_4 k_{slow}$$

$$\frac{dx_5}{dt} = x_1 \frac{x_3}{x_{3\max}} k_{C1} - x_5 k_{-C1} + x_1 \frac{x_4}{x_{4\max}} k_{A1} - x_5 k_{-A1} - x_5 k_{fast}$$

$$\frac{dx_6}{dt} = -x_6 \frac{x_2}{x_{2\max}} k_{A0} + x_7 k_{-A0} - x_6 \frac{x_2}{x_{2\max}} k_{C0} + x_8 k_{-C0} - x_6 \frac{x_7}{x_{7\max}} k_{C1} + x_9 k_{-C1} - x_6 \frac{x_8}{x_{8\max}} k_{A1} + x_9 k_{-A1}$$
$$- x_6 \frac{x_3}{x_{3\max}} k_{C1} + x_{10} k_{-C1} - x_6 \frac{x_4}{x_{4\max}} k_{A1} + x_{11} k_{-A1}$$

$$\frac{dx_7}{dt} = x_6 \frac{x_2}{x_{2\max}} k_{A0} - x_7 k_{-A0} - x_6 \frac{x_7}{x_{7\max}} k_{C1} + x_9 k_{-C1} - x_1 \frac{x_7}{x_{7\max}} k_{C1} + x_{11} k_{-C1}$$

$$\frac{dx_8}{dt} = x_6 \frac{x_2}{x_{2\max}} k_{C0} - x_8 k_{-C0} - x_6 \frac{x_8}{x_{8\max}} k_{A1} + x_9 k_{-A1} - x_1 \frac{x_8}{x_{8\max}} k_{A1} + x_{10} k_{-A1} - x_4 k_{slow}$$

$$\frac{dx_9}{dt} = x_6 \frac{x_7}{x_{7\max}} k_{C1} - x_9 k_{-C1} + x_6 \frac{x_8}{x_{8\max}} k_{A1} - x_9 k_{-A1} + x_{11} k_{fast}$$

$$\frac{dx_{10}}{dt} = x_6 \frac{x_3}{x_{3\max}} k_{C1} - x_{10} k_{-C1} + x_1 \frac{x_8}{x_{8\max}} k_{A1} - x_{10} k_{-A1} + x_5 k_{fast}$$

$$\frac{dx_{11}}{dt} = x_6 \frac{x_4}{x_{4\max}} k_{A1} - x_{11} k_{-A1} + x_1 \frac{x_7}{x_{7\max}} k_{C1} - x_{11} k_{-C1} + x_{11} k_{fast}$$

where

x_1 = *Ras**
x_2 = *SOS*
x_3 = *Ras*·SOS*
x_4 = *SOS·Ras**
x_5 = *Ras*·SOS·Ras**
x_6 = Ras^0
x_7 = Ras^0*·SOS*
x_8 = *SOS·*Ras^0
x_9 = Ras^0*·SOS·Ras**
x_{10} = *Ras*·SOS·*Ras^0
x_{11} = Ras^0*·SOS·*Ras^0

References

1. Miller, E., Antonny, B., Hamamoto, S. & Schekman, R. Cargo selection into COPII vesicles is driven by the Sec24p subunit. *Embo J* **21**, 6105-13 (2002).
2. Freedman, T.S. et al. A Ras-induced conformational switch in the Ras activator Son of sevenless. *Proc Natl Acad Sci U S A* **103**, 16692-7 (2006).